



Published in final edited form as:

Clin Cancer Res. 2014 December 15; 20(24): 6479–6494. doi:10.1158/1078-0432.CCR-14-0463.

Doxorubicin synergizes with 34.5 ENVE to enhance antitumor efficacy against metastatic ovarian cancer

Chelsea Bolyard¹, Ji Young Yoo¹, Pin-Yi Wang², Uksha Saini³, Kellie S. Rath⁴, Tim Cripe², Jianying Zhang⁵, Karuppaiyah Selvendiran³, and Balveen Kaur¹

¹Dardinger Laboratory for Neuro-oncology and Neurosciences, Department of Neurological Surgery, The Ohio State University, Columbus OH

²Center for Childhood Cancer and Blood Diseases, The Research Institute at Nationwide Children's Hospital, Columbus OH

³Division of Gynecologic Oncology, Department of Obstetrics and Gynecology, The Ohio State University, Columbus, OH

⁴Ohio Health Gynecologic Cancer Surgeons, Ohio Health Systems, Columbus, OH

⁵Center for Biostatistics, Department of Biomedical Informatics, The Ohio State University, Columbus, OH

Abstract

Purpose—Novel therapeutic regimens are needed to improve dismal outcomes associated with late-stage ovarian cancer. Oncolytic viruses are currently being tested in patients with ovarian cancer. Here we tested the therapeutic efficacy of combining doxorubicin with 34.5ENVE, an oncolytic herpes simplex virus transcriptionally driven by a modified stem cell-specific nestin promoter, and encoding for anti-angiogenic Vasculostatin-120 (VStat120) for use against progressive ovarian cancer.

Experimental Design—Anti-tumor efficacy of 34.5ENVE was assessed in ovarian cancer cell lines, mouse ascites-derived tumor cells, and primary patient ascites-derived tumor cells by standard MTT assay. The ability of conditioned medium derived from 34.5ENVE-infected ovarian cancer cells to inhibit endothelial cell migration was measured by a transwell chamber assay. Scope of cytotoxic interactions between 34.5ENVE and doxorubicin were evaluated using Chou-Talalay synergy analysis. Viral replication, HSV receptor expression, and apoptosis were evaluated. Efficacy of oncolytic viral therapy in combination with doxorubicin was evaluated *in vivo* in the murine xenograft model of human ovarian cancer.

Results—Treatment with 34.5ENVE reduced cell viability of ovarian cancer cell lines, and mouse ascites-derived and patient ascites-derived ovarian tumor cells. Conditioned media from tumor cells infected with 34.5ENVE reduced endothelial cell migration. When combined with doxorubicin, 34.5ENVE killed synergistically with a significant increase in caspase-3/7 activation,

and an increase in sub-G1 population of cells. The combination of doxorubicin and 34.5ENVE significantly prolonged survival in nude mice bearing intraperitoneal ovarian cancer tumors.

Conclusions—This study indicates significant antitumor efficacy of 34.5ENVE alone, and in combination with doxorubicin against disseminated peritoneal ovarian cancer.

Introduction

Epithelial ovarian cancer (OvCa) is the 5th most deadly cancer in women, with over 22,000 new cases and 14,000 deaths in the United States in 2013. Two-thirds of women present with progressive disease wherein the cancer has already disseminated to abdominal organs or distant sites (1). The five-year relative survival rate for these patients is less than 30% (1). Primary treatment for ovarian cancer involves cytoreductive surgery and a platinum and/or taxane chemotherapeutic regimen (2). Unfortunately, standard therapies have shown limited efficacy with nearly 70% of patients recurring with chemoresistant disease.

OvCa recurrence is often attributed to a small sub-population of cancer stem-like cells that maintain or rapidly develop resistance to chemotherapy (3). These stem-like cancer cells are critical for re-initiation of tumor growth in pre-clinical models, and are capable of serial propagation of the original tumor phenotype in animals (4, 5). Tumor cells isolated from malignant ascites have been described to be more stem-like with higher nestin expression (6, 7). Thus, a treatment regimen designed to preferentially target nestin-expressing cancer cells may have improved therapeutic efficacy and prolong survival.

The process of angiogenesis is also a key component in enabling ovarian cancer to grow and metastasize (8, 9). High levels of intra-tumoral VEGF and VEGF receptor correlate with poor patient prognosis and survival (10), and its increased expression contributes to the formation of malignant ascites, a major burden of disease (11, 12). Inhibitors of the VEGF pathway, such as bevacizumab and VEGF Trap have been shown to be effective in women with ovarian cancer in phase II and III clinical trials (reviewed in (13, 14)). We hypothesize that a treatment regimen designed to preferentially target nestin-expressing cancer cells, along with antiangiogenic therapy will have improved therapeutic efficacy and prolong survival.

Oncolytic viral (OV) therapy is a promising biological therapy that preferentially targets tumor cells for lytic destruction, while sparing normal cells (15, 16). Many different OVs have been examined for use against ovarian cancer, including oncolytic herpes simplex virus (HSV)-1; adenovirus; reovirus; and measles virus. Here we examined therapeutic efficacy of 34.5ENVE (γ 34.5-Expressed by Nestin promoter and Vasculostatin-120 Expressing) virus, an oncolytic HSV-1 that targets the transcription of the viral ICP34.5 gene to nestin-expressing cells, and encodes for Vasculostatin-120 (VStat120), a secreted antiangiogenic gene, for efficacy against ovarian cancer alone and in conjunction with doxorubicin (17–19). Our results show significant anti-tumor efficacy of 34.5ENVE against disseminated peritoneal ovarian cancer *in vivo*. Additionally, combination of 34.5ENVE with doxorubicin leads to synergistic killing of ovarian cancer cell lines and primary patient ascites-derived tumor cells *in vitro*. Treatment of mice bearing disseminated peritoneal ovarian cancer with a combination of doxorubicin and 34.5ENVE further improved antitumor efficacy. Future

testing in patients will establish the potential for use of oncolytic HSV with doxorubicin for the treatment of progressive or disseminated ovarian cancer.

Materials & Methods

Cell lines and reagents

PA-1, OV-4, OVCAR-3, SKOV3 human ovarian carcinoma cells and Vero (African green monkey kidney cells) were obtained from the ATCC (Manassas, VA). Cisplatin-resistant (A2780-CR) and cisplatin-sensitive (A2780-CS) human ovarian cancer cells were a kind gift from Dr. Rajagopalan Sridhar, (Department of Radiation Oncology, Howard University Medical School, Washington DC). SKOV3.ip1-firefly Luciferase were a kind gift from Dr. Kah-Wey Peng (20) (Mayo Clinic, Rochester, MN). PA-1 and OV-4 were maintained in Dulbecco's modified Eagle's medium supplemented (DMEM) with 10% fetal bovine serum (FBS) and penicillin/streptomycin (100 U/mL and 100 µg/mL) at 37°C and 5% CO₂. OVCAR-3, SKOV3 and SKOV3-ip1-fLuc were maintained in α -Minimal Essential Medium (α MEM) supplemented with 20% FBS and penicillin/streptomycin (100 U/mL and 100 µg/mL) at 37°C and 5% CO₂. Human dermal microvessel endothelial cells (HDMEC) were obtained from ScienCell, and maintained at low passage number in Endothelial Basal Media with supplements (ScienCell, Carlsbad, CA) and penicillin/streptomycin (100 U/mL and 100 µg/mL) at 37°C and 5% CO₂. Chinese hamster ovary (CHO) cells negative for expression of HSV-1 entry receptors (CHO-K1) and CHO-K1 cells transduced to express human nectin-1 (CHO-N1) or nectin-2 (CHO-N2) were kind gifts from Patricia G. Spear (Northwestern University, IL, USA)(21, 22). CHO-K1 cells stably expressing human HVEM (CHO/A) were as described (23). CHO cells were cultured in F12 medium containing 10% FBS, penicillin/streptomycin (100 U/mL and 100 µg/mL) and G418 at 37°C and 5% CO₂. Doxorubicin was obtained from Sigma-Aldrich (St. Louis, MO), and dissolved in DMSO, and then further diluted described in PBS for use.

Viruses

Construction of 34.5ENVE has been previously described (17). Briefly, to generate 34.5ENVE, an expression cassette encoding *Vstat120* gene regulated by the viral IE4/5 promoter with ICP34.5 regulated by a nestin enhancer driven promoter was inserted into fHSVQ backbone using HSVQuik technology (24). Revertant ENVE was created by removing the expression cassette containing the ICP34.5 and VStat120 gene by recombination. Viruses were propagated in Vero cells. Three days after infection, Vero cells and media were harvested and subjected to three cycles of freezing in liquid nitrogen and thawing at 37°C to liberate virions. Cell debris was cleared by centrifugation (400 g, 20 min at 4°C). Virus was pelleted from resultant supernatant by centrifugation at 13,000 g for 1 hour. Virus titer was determined via plaque-forming assay in Vero cells, with plaque-forming units (PFU) assessed 3 days after infection (24).

Cell Viability Assay and Chou-Talalay Analysis

Cancer cells were seeded into a 96-well plate (in 2% FBS media in 100µl volume), and were treated with vehicle or doxorubicin for 18 hours followed by drug wash out, and then virus infection. Three days after infection, cell viability was measured using a standard MTT

assay (Roche Applied Sciences, Indianapolis IN). For synergy analysis, dose response curves and 50% effective dose (ED50) values were determined for each individual treatment (drug or virus). Fixed ratios of ED50 of drug and/or virus were then used to treat the cells, either individually (as controls) or in combination. CompuSyn software (ComboSyn, Inc. Paramus, NJ) program algorithm assessed the Combination Index (CI). Combined dose-response curves were fitted to Chou-Talalay lines, which are derived from the law of mass action. $CI < 1$ indicates synergistic interaction, whereas $CI > 1$ is antagonistic, and $CI = 1$ is additive (25–28).

RT- PCR

To measure relative nestin expression, RNA was purified from cell pellets (QIAGEN RNeasy, Qiagen, Valencia, CA), per manufacturer's instructions. cDNA was generated (SuperScript Reverse Transcriptase, Life Technologies, Grand Island, NY), and nestin expression was measured via quantitative RT-PCR (Mastercycler ep realplex, Eppendorf, Hauppauge, NY) using SYBR Green (Applied Biosystems, Grand Island, NY). GAPDH was used as an internal control. Primer sequences: GAPDH, forward, 5'-GGAGTCAACGGATTTGGTCG-3'; reverse, 5'-GGAATCATATTGGAACATGTAAACC-3'. Nestin, forward, 5'-TCCAGGAACGGAAAATCAAG-3; reverse, 5'-GCCTCCTCATCCCCTACTTC-3'. To evaluate murine cell contamination of mouse ascites-derived tumor cells, mouse and human beta actin was probed. Primer sequences: mouse beta-actin, forward, 5'-CCTTCTTGGGTATGGAATCCTG-3'; reverse, 5'-GGCATAGAGGTCTTTACGGATG-3'. Human beta actin, forward, 5'-CACACTGTGCCCATCTATGAGG-3'; reverse, 5'-CGCGCTCAGTGAGGATCTTC-3'. TissueScanqPCR Array Ovarian Cancer Disease Panel III (Origene, Rockville MD) was used to assess nestin expression in 48 human samples. Disease Panel contained 48 samples from pathologist-verified tissue cDNA including 6 normal (from patients with endometriosis, carcinoma of the bladder, or leiomyoma of the myometrium), 14 Stage I, 5 Stage II, 22 Stage III and 1 Stage IV sample.

Generation of concentrated conditioned media

To generate concentrated conditioned media, ovarian cancer cells were infected with the indicated oncolytic viruses (OV) at a multiplicity of infection (MOI) of 2 (two infectious viral particle per cell). One hour post-infection, unbound virus was washed away, and serum-free media was added. Twelve to 14 hours post-infection, conditioned media was harvested, treated with 0.4% human IgG to neutralize contaminating virus, and centrifuged for 1 hour at 13,000 rpm to pellet any virus in the media prior to being concentrated 100-fold using 50,000 kDa Amicon Ultra centrifugal concentration filters (Millipore, Billerica, MA).

In Vitro Endothelial Cell Migration Assays

Endothelial cell migration assays were performed using a modified Boyden chamber assay similar to previous reports (17, 18). Transwell membranes (8 μ M, Corning Costar, Cambridge, MA) were pre-coated on the underside with 5 μ g/mL fibronectin (Millipore, Billerica, MA) in PBS. Migration of serum-starved HDMEC towards conditioned medium was measured using transwell chambers. HDMEC were plated in the upper chamber, and

cells were allowed to migrate for twelve hours, at which point membranes were fixed in 1% glutaraldehyde and stained with 0.5% crystal violet; unmigrated cells were removed from top chamber (using cotton swab). Images of the membranes were obtained at 20x magnification, and quantified by counting 5 fields of view/well (n=3/group).

Viral Replication Assay and Viral Burst Assay

Cells were treated with doxorubicin for 18 hours at indicated concentrations. Drug was then washed out, and cells were infected at an MOI of 0.001 (for replication assay) or MOI of 1 (for burst assay) in 2% FBS media. Infection proceeded for 1 hour, and then unbound virus was washed away and fresh 2%FBS media was added to each well. Cells were harvested at indicated time points post-infection, and titers were determined by standard plaque assay on Vero cells (24).

Immunoblots

Immunoblots were probed with rabbit anti-N-terminal BAI1(29) to probe for VStat120, mouse anti-human GAPDH (Abcam, Cambridge, MA), or mouse anti-ICP4 (Abcam, Cambridge, MA) antibodies, followed by goat anti-rabbit (Dako, Carpinteria, CA) or sheep anti-mouse (Amersham Biosciences, Pittsburgh, PA) secondary antibodies.

Assay of Caspase-3/7 Activity

Cells were seeded onto 96-well plates (in 2% FBS media in 100µl volume), and were treated with drug, virus or combination at indicated concentrations or MOI. Caspase-3/7 activity per µg protein was evaluated using Caspase-Glo 3/7 Assay Kit (Promega, Madison, WI) and BCA Protein Assay kit (Thermo Scientific, Rockford IL) according to manufacturer's instruction. For caspase inhibition experiments, 15µM of caspase inhibitor ZVAD-FMK (Promega, Madison, WI) was added in tandem with each treatment.

Animal experiments

All animal experiments were performed in accordance with the Subcommittee on Research Animal Care at The Ohio State University guidelines, and have been approved by the institutional review board. Six- to eight-week-old female athymic nu/nu mice (18–25 grams, Charles River Laboratories, Frederick, MD), were injected intraperitoneally with 2×10^6 SKOV3.ip1-fLuc cells in 500 ul sterile saline. All treatment injections with doxorubicin, virus, or mock were administered intraperitoneally in 100 ul volume. Mice were sacrificed upon significant weight gain due to ascites accumulation, development of significant jaundice or wasting, or development of necrotic subcutaneous lesion at injection site.

Cancer cell isolation from murine ascites

To isolate cancer cells from mice ascites were collected via intraperitoneal draining using 20G needle from tumor bearing mice with obvious disseminated peritoneal disease. Upon collection, ascites volume was increased to 30 mL using PBS, and then centrifuged to pellet all cells. Cell pellet was resuspended in 5 mL of ammonium chloride red blood cell lysis buffer (StemCell Technologies, Vancouver, British Columbia, Canada); lysis proceeded at room temperature for 5 minutes with rocking. Remaining tumor cells and contaminating

immune cells were plated in 20% FBS α -MEM, and incubated for 2–3 days at 37°C in 5% CO₂. Samples were confirmed for lack of contaminating murine cells using RT-PCR probing for murine specific beta actin, and then used for experiments as indicated.

Patient ascites-derived primary ovarian carcinoma cell sample isolation

Primary ovarian carcinoma cell samples used in this study were isolated from human ascites collected at the time of debulking surgery from patients with high grade serous ovarian carcinoma. (See Supplementary Table 1 for details about each specimen, including patient age, histological subtype and cancer stage grouping). All patients signed consent forms, and the use of patient samples was approved under the Ohio State University Human Investigations Committee (IRB # 2004C0124). Routine histopathological examination of formalin-fixed paraffin-embedded tissue from each patient (carried out at the hospital) was followed, and the ascites from confirmed predominant high grade serous histological subtype was used for further experiments. Equal volume of patient ascites and warmed RPMI with 20% FBS was plated in T75 flasks (Corning, Tewksbury, MA) and incubated at 37°C, with 5% CO₂ and 95% humidified air (30). Fresh medium was replaced 3 to 5 days after initial plating, and every 4 to 5 days until the cells approached confluence. The cells were frozen in RPMI with 10% FBS and 10% glycerol in liquid nitrogen for future use. Characterization for the confirmation of the presence of tumor cells was done using antibodies for pan-cytokeratin (Abcam, Cambridge, MA), vimentin (Abcam, Cambridge, MA) and CD14 (Abcam, Cambridge, MA), with DAPI counterstain (Vector Labs, Burlingame, CA). Pan-cytokeratin^{+ve}/CD14^{-ve} and Vimentin^{+ve} cells have been previously characterized as ovarian cancer cells; co-expression of vimentin and pan-cytokeratin is frequently observed in ovarian cancer cells (30–33). Cultures with >95% pan-cytokeratin^{+ve} and vimentin^{+ve} and CD14^{-ve} were used for future experiments. All the experiments were carried out using early cells passage cells.

(34, 35) Flow Cytometry Analysis of HSV receptor expression

SKOV3 cells were treated with 40 nM doxorubicin for 18 hours prior to harvesting. Anti-human nectin-1 (R1.302.12, sc-6918, Santa Cruz Biotechnology, Santa Cruz CA), nectin-2 (R2.525, sc-32804, Santa Cruz Biotechnology), HVEM (CW10, sc-21718, Santa Cruz Biotechnology) and FITC-conjugated goat anti-mouse IgG (BD Biosciences, San Jose CA) were used for HSV entry receptor staining.

Luciferase Imaging

Luciferase imaging was performed using Xenogen IVIS *in vivo* imaging system (Perkin Elmer, Waltham, MA). Luciferin was used at *in vivo* concentration as indicated by manufacturer's instructions (Perkin Elmer, Waltham, MA).

Statistics

For normally distributed measurements (or data transformed to normal), a two-sample *t* test was used to compare the means of two independent groups. ANOVA models or linear models were used to compare the mean of multiple groups, or to include two or more factors. Two-way ANOVA models with the interaction term were used to evaluate the

synergistic effect between two treatments (e.g. Doxorubicin and 34.5ENVE). For survival data, survival rates were estimated by Kaplan-Meier method, and the survival curves were displayed and compared among groups by Log rank test. All tests were two-sided. P values were adjusted for multiple comparisons using Holm's procedure. An adjusted P value of 0.05 or less was considered statistically significant

Results

Ovarian cancer cells are sensitive to killing by 34.5ENVE oncolytic virus, and mediate increased 34.5ENVE replication

The genetic structures of the oncolytic viral (OV) vectors used in this study have been previously described (17, 24, 36), and are outlined in Figure 1A. Briefly, 34.5ENVE virus is an oncolytic HSV-1 with a disrupted ICP6 gene and deletions of both native copies of the ICP34.5 gene. It then has one copy of ICP34.5 driven by a modified nestin promoter reintroduced into the backbone, and also expresses antiangiogenic VStat120 driven by an immediate early viral promoter (called IE4/5)(17). A rescue virus, called revertant ENVE, was generated by removal of the inserted nestin-driven ICP34.5 and IE4/5-driven VStat120 expression cassette from the 34.5ENVE backbone. To determine if OvCa cell lines were sensitive to 34.5ENVE and revertant ENVE, the indicated cells were infected with virus at increasing multiplicity of infection (MOI), and cell viability was measured by standard MTT assay. Figure 1B shows sensitivity of OvCa cell lines to killing by both 34.5ENVE and revertant ENVE. The two-way ANOVA test indicated that in four out of six cell lines tested there is an overall significant difference between sensitivity to killing by revertant ENVE and 34.5ENVE (Figure 1B). The two cell lines, A2780CR and A2780CS, which only showed a trend towards overall significant difference, were also extremely sensitive to virus killing relative to the other four cell lines, even with the 34.5-deleted revertant ENVE. OvCa cell lines were also conducive to viral replication, with 34.5ENVE replicating better than revertant ENVE. Figure 1C shows viral replication after 72 hours in several cell lines as measured by standard plaque assay (24)(students t test; *, $p < 0.05$, **, $p < 0.001$; ***, $p < 0.0001$).

Mouse ascites-derived and patient ascites-derived tumor cells express increased nestin expression, and sensitivity to 34.5ENVE

To evaluate if increased sensitivity to OV correlated with nestin expression, we compared sensitivity of SKOV3 cells grown *in vitro* to SKOV3 cells harvested from murine ascites which develop in mice after tumor implantation. Tumor cells isolated from malignant ascites have been described to be more stem-cell like with higher nestin expression (6, 7). Consistent with published reports, *ex vivo* SKOV3 cells harvested from ascites from three individual mice (Figure 2A and B, "ascites-1", ascites-2" and "ascites-3") had more than a 10-fold increase in nestin expression compared to SKOV3 cells grown *in vitro* as determined by RT-PCR (Figure 2A). Along with increased nestin expression, the *ex vivo* ascites-derived tumor cells were significantly more sensitive overall killing by 34.5ENVE compared to revertant ENVE (Figure 2B; linear models were used to compare the means of two groups).

While SKOV3, A2780, and OVCAR3 cells were originally isolated from ovarian cancer patients, and are identified as such according to the ATCC, molecular profiling of commonly used ovarian cancer cells revealed some differences between the molecular profile of commonly-used ovarian cancer cell lines, and that of most high grade serous ovarian cancer tissue derived from patients (37). Thus we analyzed sensitivity of primary ovarian cancer patient ascites-derived tumor cells to 34.5ENVE or revertant ENVE. Ascites from ovarian cancer patients (de-identified patient numbers 140, 163, 179, 195; described in Supplementary Table 1) were isolated, and cultured as described in the Materials and Methods section. The ascites isolated tumor cell culture displayed cobblestone monolayer morphology as described (38) (Supplementary Figure 1). The characterization of the cultures was carried out using immunocytochemistry and immunofluorescence using a panel of antibodies to detect expression of pan-cytokeratin, vimentin and CD14 (Supplementary Figure 1). Pan-cytokeratin^{+ve}/CD14^{-ve} and Vimentin^{+ve} cells have been previously characterized as ovarian cancer cells (30).

RT-PCR for nestin gene expression revealed that these ascites-derived tumor cells had increased nestin expression 10-to-100-fold as compared to normal ovarian tissue obtained from tissue qPCR array (from patients with endometriosis, carcinoma of the bladder, or leiomyoma of the myometrium, n=6) (Figure 2C). TissueScanqPCR Array Ovarian Cancer Disease Panel III (Origene, Rockville MD) was used to assess nestin expression in 48 human samples. Analysis of primary patient cDNA samples indicated that nestin expression increases with tumor grade (Figure 2D; ANOVA models used to compare the mean of multiple groups; p value adjusted by Holm's procedure). Consistent with the increased nestin expression, the primary patient ascites-derived tumor cells also had increased overall sensitivity to 34.5ENVE-mediated killing compared to revertant ENVE (Figure 2E; linear models used to compare the means of two groups).

Antiangiogenic protein VStat120 is produced by 34.5ENVE after infection of OvCa, and reduces endothelial cell migration *in vitro*

We examined the ability of OvCa cells infected with 34.5ENVE to produce and secrete VStat120 by Western blot analysis. Figure 3A (middle panel) shows presence of Vasculostatin-120 in cell lysates from a panel of OvCa cell lines infected with 34.5ENVE (indicated with arrow). Furthermore, 34.5ENVE infection yielded a more robust production of viral immediate early protein ICP4 (Figure 3A, top panel). The presence of secreted VStat120 was also confirmed by western blot analysis of concentrated conditioned medium (CM) derived from SKOV3 and patient ascites-derived cells infected with 34.5ENVE, revertant ENVE or mock (Figure 3B).

To assess the functionality of secreted VStat120 produced by infected OvCa cells, we compared the effect of CM from SKOV3 or primary patient ascites infected with the indicated virus, or PBS on endothelial cells migration in a modified Boyden chamber. Briefly, CM from 34.5ENVE-, revertant ENVE-, or mock-infected cells was added to the bottom chamber, and migration of HDMEC towards the bottom chamber was quantified. There was a significant reduction in endothelial cell migration upon treating with VStat120-containing CM from either infected SKOV3 (26.5% reduction, p=0.0204) or patient ascites

(29.6% reduction, $p=0.014$) (Figure 3C; ANOVA models used to compare the mean of multiple groups; p value adjusted by Holm's procedure).

Therapeutic efficacy of 34.5ENVE against disseminated peritoneal ovarian cancer *in vivo*

To test therapeutic efficacy of 34.5ENVE against ovarian cancer *in vivo*, mice with established intraperitoneal SKOV3 ovarian tumors were treated with PBS, revertant ENVE or 34.5ENVE (5×10^5 plaque-forming units (PFU)) three times, on 8, 16 and 23 days after tumor cell implantation (Figure 4A; virus treatment indicated with arrows). Kaplan-Meier survival analysis revealed a significant increase in median survival time of mice treated with oncolytic virus (OV) as compared to PBS, with a greater prolonging of survival in mice treated with 34.5ENVE as compared to revertant ENVE-treated animals (Figure 4A; s compared among groups by Log rank test). Median survival was 63 days for 34.5ENVE-treated mice, 49 days for revertant ENVE-treated mice, and 37 days for PBS treated mice. (Figure 4A; $p < 0.001$)

Luciferase expression by SKOV3 cells permitted live imaging of mice to monitor disease progression using an *in vivo* imaging system (IVIS). There was a significant reduction in luciferase activity (as indicated by relative light units (RLU) in photons/second) in 34.5ENVE-treated cohort 28 days after tumor implantation, as compared to PBS (Figure 4B, luminescent images; Figure 4C, quantification of luminescent output, $p=0.0342$ between PBS and 34.5ENVE; ANOVA models used to compare the mean of multiple groups; p value adjusted by Holm's procedure). Interestingly, all mice showed a delayed development of a subcutaneous tumor at the site of tumor injection. Since virus treatment was administered via intraperitoneal injection on the opposite side of the abdomen, this subcutaneous nodule served as an untreated control tumor in each mouse. Eight of eight mice treated with PBS developed aggressive ascites by the time of sacrifice, whereas only four of eight mice treated with revertant ENVE developed ascites (Figure 4D). Only two of the eight mice treated with 34.5ENVE showed the development of ascites at time of death, while the other six mice were sacrificed due to the growth of the untreated subcutaneous tumor. Gross histology of the ascites-free 34.5ENVE treated mice (6/8) revealed that they were free of disseminated intraperitoneal metastatic tumor seeding (Figure 4D; tumor nodules indicated with white asterisks).

Doxorubicin synergizes with 34.5ENVE to kill ovarian cancer cells *in vitro* and *in vivo*

To evaluate impact of doxorubicin treatment in combination with 34.5ENVE, we determined what treatment schedule was most effective for combining the two agents. Briefly, SKOV3 cells were treated with a fixed concentration of doxorubicin (100 nM) and with varying doses of 34.5ENVE administered 18 hours before doxorubicin, at the same time, or 18 hours after doxorubicin. Viability was measured 3 days after infection by MTT assay. Impact of doxorubicin and 34.5ENVE on cytotoxicity is depicted in Figure 5A. Treatment with doxorubicin prior to 34.5ENVE (far right panel) showed an increase in cell killing compared to 34.5ENVE alone, thus all subsequent experiments were performed with this treatment schedule. Linear models were used to compare the means of two groups; $p < 0.001$ comparing 34.5ENVE treatment to 34.5ENVE with doxorubicin.

We then measured sensitivity of doxorubicin-treated OvCa cell lines to 34.5ENVE. Cells were treated with doxorubicin for 18 hours followed by drug wash-out, and infected with 34.5ENVE for 72 hours. Viability was measured by MTT assay. Reduction in viability by either agent alone was quantified (D1: reduction in cell viability by doxorubicin; D2: reduction in cell viability by 34.5ENVE). Reduction in viability by combination of doxorubicin and 34.5ENVE treatment was also quantified (called D3). Additive effect was calculated as [D1+D2]. Synergistic effect was calculated as [D3-(D1+D2)]. In all 6 ovarian cancer cell lines, treatment of cells with both 34.5ENVE and doxorubicin resulted in more-than-additive cell killing (Figure 5B; two-way ANOVA models with the interaction term were used to evaluate the synergistic effect between two treatments). Since this suggested synergistic cell killing, we next examined the ability of doxorubicin to synergize with 34.5ENVE using the Chou-Talalay synergy analysis method as described (25, 26, 28, 39). This analysis is frequently utilized to investigate synergy between anti-cancer killing of agents (39–41). Briefly, the 50% effective dose (ED50) of doxorubicin and 34.5ENVE were each defined as the dosage yielding 50% cell viability, as compared to untreated controls. To evaluate if the combination resulted in synergistic cell killing, the cells were treated with doxorubicin, followed by drug wash-out, and then treated with 34.5ENVE. Concentrations of doxorubicin and 34.5ENVE were serially diluted at fixed ratios of 0.0625, 0.125, 0.25, 0.5, 1, 2 and 4 times their ED50. Cell viability was measured 72 hours after virus infection. The viability data was utilized to calculate the Combination Index (CI) via Compusyn program. CI<1 indicates synergistic interaction, whereas CI>1 is antagonistic, and CI=1 is additive. Doxorubicin and 34.5ENVE combination therapy killed the ovarian cancer cells synergistically in all cell lines at most fractions affected (Fa), as indicated by the Combination Index (CI) (Figure 5C). In a parallel experiment, we tested sensitivity of primary patient ascites-derived tumor cells to doxorubicin alone, and in combination with 34.5ENVE. Consistent with the cell line data, synergistic cell killing was observed between doxorubicin and 34.5ENVE in primary patient ascites-derived cell samples (Figure 5D).

Next, we tested the *in vivo* relevance of this synergistic cell killing of doxorubicin in combination with 34.5ENVE. Mice with established intraperitoneal tumors were treated with a single dose of doxorubicin (10 μ g/gram body weight) eight days post tumor cell implantation. One day later, mice were treated with a single injection of 34.5ENVE (5 \times 10⁵ PFU). Median survival was 58 days for doxorubicin with 34.5ENVE treatment, 47 days for 34.5ENVE alone, 47 days for doxorubicin alone, and 32.5 days for PBS-treated (Figure 5E). Kaplan-Meier survival analysis revealed a significant increase in survival of mice treated with combination therapy of doxorubicin with 34.5ENVE as compared to either agent alone (Figure 5E; survival curves compared among groups by Log rank test; p<0.001).

Combination therapy with doxorubicin and 34.5ENVE does not alter viral infection or replication, but increases and is dependent upon caspase-3/7 activation

Doxorubicin and 34.5ENVE combination treatment synergistically kills OvCa according to Chou-Talalay synergy analysis and *in vivo* results. To test if doxorubicin affected virus replication or infection, we first measured its impact on viral transduction over time by measuring increase in GFP-positive infected cells by FACS analysis. Figure 6A shows no increase in the relative percentage of GFP-positive cells at indicated time points after

treatment with increasing concentrations of doxorubicin. Consistent with this observation, there was no change in HSV-1 receptor expression (nectin-1, nectin-2, herpes virus entry mediator (HVEM)) in SKOV3 cells treated with 40 nM doxorubicin for 18 hours (Figure 6B). These results suggest that the increased cell killing was not due to increase in virus transduction after treatment of cells with doxorubicin. Furthermore, replication assays and viral burst assays in the presence or absence of doxorubicin showed no change in viral replication over time with increasing concentrations of doxorubicin treatment (Figure 6C, replication assay; Figure 6D, viral burst assay). These results suggest that the increased cell killing was not due to increase in virus replication after treatment of cells with doxorubicin.

Doxorubicin is known to induce apoptosis in ovarian cancer cells. To evaluate if virus treatment increased apoptosis in ovarian cancer cells, we first measured DNA content via flow cytometry to examine changes in the sub-G1 apoptotic population of cells after a 24 hour treatment with single agent or combination therapy. Treatment with both doxorubicin and 34.5ENVE increased sub-G1 apoptotic population of cells, as compared to either therapy alone (Figure 6E, representative images). We then measured relative caspase-3/7 activation in cells treated with doxorubicin alone or in combination with 34.5ENVE after 24 hours (Figure 6F, normalized to untreated control; ANOVA models used to compare the mean of multiple groups; p value adjusted by Holm's procedure). Combination therapy of doxorubicin (160 nM) and 34.5ENVE (MOI=0.04) significantly increased caspase-3/7 activation in SKOV3 cells over either individual therapy, indicating that the synergistic killing may be mediated via increased apoptosis. Pretreatment of SKOV3 cells with pan-caspase inhibitor ZVAD-FMK (15 μ M) effectively blocks caspase activation (Figure 6G). Figure 6G shows relative light units indicating caspase-3/7 activation in cells treated with doxorubicin alone or in combination with 34.5ENVE with or without ZVAD-FMK. Our data indicates significant increase in caspase activation in combination therapy. Consistent with these findings, the synergistic interaction between doxorubicin and 34.5ENVE can be ablated by treatment with caspase inhibitor ZVAD-FMK as assessed by Chou-Talalay synergy analysis (Figure 6H; CI<1 indicates synergistic interaction; CI>1 is antagonistic; CI=1 is additive).

Discussion

Several different oncolytic HSV-1 derived viruses, including HSV1716 and fusogenic Synco-2D, have been shown to be effective against metastatic ovarian cancer in pre-clinical studies (42–44). Patients with late-stage or recurrent ovarian cancer are currently being recruited for clinical trials to evaluate the use of oncolytic measles virus, or Reovirus with or without paclitaxel (NCT00408590, NCT01199263). Here we evaluated therapeutic efficacy of 34.5ENVE against disseminated intraperitoneal ovarian cancer in mice. All oncolytic HSV tested in patients to date have been deleted for both copies of the viral ICP34.5 gene. ICP34.5 plays a crucial role in modulating the cellular PKR-driven antiviral immune response (45). It also inhibits the induction of cellular autophagy, another anti-viral defense response (46); and is involved in recruiting PCNA to sites of virus replication (47). HSV-1 vectors deleted for ICP34.5 are safe for intracerebral administration, but the resulting virus is severely attenuated for replication (48–50). 34.5ENVE is designed to reintroduce ICP34.5 gene under the regulation of a modified nestin promoter resulting in an OV with increased

potency in nestin-positive cells (17). Nestin is a marker of stem cells, and its expression has been associated with cancer stem-like cells in several malignancies including glioma, ovarian, and pancreatic cancers (4, 5, 51–53). Here we tested the sensitivity of primary patient and experimental mouse ascites-derived tumor cells to 34.5ENVE. We also compared the nestin expression of tumor cells derived from ascites that developed in the experimental mouse model of progressive ovarian cancer to the parent cell line grown *in vitro*. Consistent with previous reports describing the presence of cancer stem-like cells in ascites, we found elevated nestin expression in ascites-derived tumor cells (4, 5). These cells were significantly more sensitive to killing by 34.5ENVE than the parent cell line. Additionally, primary patient ascites-derived tumor cells displayed high levels of nestin gene expression, and were sensitive to 34.5ENVE-mediated oncolysis. This is the first study, to our knowledge, to evaluate the use of oncolytic HSV-1 against tumor cells derived from freshly-isolated malignant ovarian cancer ascites. In addition to expressing a nestin-driven ICP34.5, 34.5ENVE also encodes for Vstat120, a potent antiangiogenic fragment derived from the extracellular fragment Brain Angiogenesis Inhibitor 1 (BAI1). In our study, we observed reduced endothelial cell migration *in vitro*, and a decrease in tumor dissemination-associated ascites *in vivo*. The antiangiogenic properties of Vstat120 have been attributed to five thrombospondin type 1 domains contained within it (19). The use of thrombospondin-1 (TSP1) mimetic proteins for ovarian cancer has shown promising results in preclinical models, and treatment with TSP1 mimetics such as ABT-510 reduced tumor growth, ascites fluid and intraperitoneal dissemination, in an orthotopic, syngenic model of ovarian cancer (54, 55). However, clinical testing in patients with advanced soft tissue sarcoma, renal cell carcinoma and melanoma showed disappointing efficacy results with use of ABT-510 as a single agent, and suggested testing it in combination with other agents in future trials (56, 57). Interestingly 34.5ENVE-treated animals showed a reduction in the formation of ascites along with a reduction in intraperitoneal seeding of tumor cells. The direct cytolytic effects of the virus along with the continuous release of antiangiogenic Vstat120 from infected cells provide 34.5ENVE with a two pronged therapeutic approach not achievable by repeatedly administration of an antiangiogenic peptide.

Here we tested the impact of combining 34.5ENVE with doxorubicin. Combination of oncolytic HSV-1 with DNA-damaging agents has been shown to improve viral replication and anti-tumor efficacy in several different cancer models (25, 50, 58,59). Here we found that doxorubicin and 34.5ENVE killed OvCa cell lines and patient ascites-derived tumor cells synergistically without affecting virus entry or replication. Combination therapy increased sub-G1 population of apoptotic cells more than either therapy alone. We also found that combination therapy significantly increased caspase-3/7 activation and apoptosis. Blockade of effector caspases ablated the synergistic interaction between doxorubicin and 34.5ENVE, suggesting that the combination effect was mediated by caspase activation and apoptosis. This is consistent with previous reports wherein chemotherapy treatment was shown to select for chemotherapy-resistant cancer stem cells which can then become susceptible to a nestin-driven oncolytic HSV-1 vector (52, 60). Doxorubicin-based therapies are frequently prescribed for ovarian cancer patients who have developed resistance to taxane- and platinum-containing agents. The finding that 34.5ENVE synergizes with this

agent underscores the potential significance of testing oncolytic HSV therapy in conjunction with doxorubicin for ovarian cancer patients.

Interestingly, in a previous report, doxorubicin in combination with HSV1716 (an oncolytic HSV-1 derived virus deleted for ICP34.5) was found to have an additive effect in non-small cell lung cancer (61). Consistent with these results, we found that combining doxorubicin and 34.5ENVE at the same time yielded additive results. However, altering our treatment schedule yielded different results, indicating that scheduling optimization will be critical for evaluating therapeutic combinations including OV therapy. Furthermore, mutations in oncolytic virus backbones have a critical impact on how cellular signaling is altered in different cell types. This highlights the importance of testing efficacy of individual oncolytic viruses alone and in combination with chemotherapy in preclinical models prior to testing in patients. TSP1 mimetic ABT-510 has been shown to induce apoptosis in ovarian cancer cells, and it is interesting to speculate if the apoptotic effect of 34.5ENVE on ovarian cancer cells depends on Vstat120 expression.

In conclusion, we report that doxorubicin-based chemotherapy, a standard of care for recurrent or refractive ovarian cancer, can be combined with 34.5ENVE to synergistically kill ovarian cancer cells, and combination therapy results in prolonged survival and reduced tumor and ascites burden in the *in vivo* model of ovarian cancer. This may be a potential combination therapy for use in the clinic for patients with recurrent or refractive ovarian cancer.

Supplementary Material

Refer to Web version on PubMed Central for supplementary material.

References

1. SEER Cancer Statistics Review, 1975–2010. Bethesda, MD: National Cancer Institute; 2013. [cited 2013]. Available from: http://seer.cancer.gov/csr/1975_2010/, based on November 2012 SEER data submission, posted to the SEER web site
2. Network NCC. NCCN Guidelines Version 2.2013; Epithelial Ovarian Cancer/Fallopian Tube Cancer/Primary Peritoneal Cancer. 2013. [cited 2013]. Available from: http://www.nccn.org/professionals/physician_gls/pdf/ovarian.pdf
3. Zhan Q, Wang C, Ngai S. Ovarian cancer stem cells: a new target for cancer therapy. *BioMed research international*. 2013; 2013:916819. Epub 2013/03/20. 10.1155/2013/916819 [PubMed: 23509802]
4. Zhang S, Balch C, Chan MW, Lai HC, Matei D, Schilder JM, et al. Identification and characterization of ovarian cancer-initiating cells from primary human tumors. *Cancer research*. 2008; 68(11):4311–20. Epub 2008/06/04. CAN-08-0364. 10.1158/0008-5472 [PubMed: 18519691]
5. Gao MQ, Choi YP, Kang S, Youn JH, Cho NH. CD24+ cells from hierarchically organized ovarian cancer are enriched in cancer stem cells. *Oncogene*. 2010; 29(18):2672–80. Epub 2010/03/02. 10.1038/onc.2010.35 [PubMed: 20190812]
6. Meng E, Long B, Sullivan P, McClellan S, Finan MA, Reed E, et al. CD44+/CD24– ovarian cancer cells demonstrate cancer stem cell properties and correlate to survival. *Clinical & experimental metastasis*. 2012; 29(8):939–48. Epub 2012/05/23. 10.1007/s10585-012-9482-4 [PubMed: 22610780]
7. Luo L, Zeng J, Liang B, Zhao Z, Sun L, Cao D, et al. Ovarian cancer cells with the CD117 phenotype are highly tumorigenic and are related to chemotherapy outcome. *Experimental and*

- molecular pathology. 2011; 91(2):596–602. Epub 2011/07/27. 10.1016/j.yexmp.2011.06.005 [PubMed: 21787767]
8. Brown MR, Blanchette JO, Kohn EC. Angiogenesis in ovarian cancer. *Bailliere's best practice & research Clinical obstetrics & gynaecology*. 2000; 14(6):901–18. Epub 2001/01/06. 10.1053/beog.2000.0134
 9. Alvarez AA, Krigman HR, Whitaker RS, Dodge RK, Rodriguez GC. The prognostic significance of angiogenesis in epithelial ovarian carcinoma. *Clinical cancer research: an official journal of the American Association for Cancer Research*. 1999; 5(3):587–91. Epub 1999/04/01. [PubMed: 10100710]
 10. Engels K, du Bois A, Harter P, Fisseler-Eckhoff A, Kommoss F, Stauber R, et al. VEGF-A and i-NOS expression are prognostic factors in serous epithelial ovarian carcinomas after complete surgical resection. *Journal of clinical pathology*. 2009; 62(5):448–54. Epub 2009/01/08. 10.1136/jcp.2008.063859 [PubMed: 19126566]
 11. Nagy JA, Masse EM, Herzberg KT, Meyers MS, Yeo KT, Yeo TK, et al. Pathogenesis of ascites tumor growth: vascular permeability factor, vascular hyperpermeability, and ascites fluid accumulation. *Cancer research*. 1995; 55(2):360–8. Epub 1995/01/15. [PubMed: 7812969]
 12. Nagy JA, Morgan ES, Herzberg KT, Manseau EJ, Dvorak AM, Dvorak HF. Pathogenesis of ascites tumor growth: angiogenesis, vascular remodeling, and stroma formation in the peritoneal lining. *Cancer research*. 1995; 55(2):376–85. Epub 1995/01/15. [PubMed: 7529135]
 13. Burger RA. Overview of anti-angiogenic agents in development for ovarian cancer. *Gynecologic oncology*. 2011; 121(1):230–8. Epub 2011/01/11. 10.1016/j.ygyno.2010.11.035 [PubMed: 21215996]
 14. Schmitt J, Matei D. Targeting angiogenesis in ovarian cancer. *Cancer treatment reviews*. 2012; 38(4):272–83. Epub 2011/07/19. 10.1016/j.ctrv.2011.06.004 [PubMed: 21764518]
 15. Wojton J, Kaur B. Impact of tumor microenvironment on oncolytic viral therapy. *Cytokine & growth factor reviews*. 2010; 21(2–3):127–34. Epub 2010/04/20. 10.1016/j.cytogfr.2010.02.014 [PubMed: 20399700]
 16. Haseley A, Alvarez-Breckenridge C, Chaudhury AR, Kaur B. Advances in oncolytic virus therapy for glioma. *Recent patents on CNS drug discovery*. 2009; 4(1):1–13. [PubMed: 19149710]
 17. Yoo JY, Haseley A, Bratasz A, Chiocca EA, Zhang J, Powell K, et al. Antitumor efficacy of 34.5ENVE: a transcriptionally retargeted and “Vstat120”-expressing oncolytic virus. *Molecular therapy: the journal of the American Society of Gene Therapy*. 2012; 20(2):287–97. Epub 2011/10/28. 10.1038/mt.2011.208 [PubMed: 22031239]
 18. Hardcastle J, Kurozumi K, Dmitrieva N, Sayers MP, Ahmad S, Waterman P, et al. Enhanced antitumor efficacy of vasculostatin (Vstat120) expressing oncolytic HSV-1. *Molecular therapy: the journal of the American Society of Gene Therapy*. 2010; 18(2):285–94. Epub 2009/10/22. 10.1038/mt.2009.232 [PubMed: 19844198]
 19. Kaur B, Brat DJ, Devi NS, Van Meir EG. Vasculostatin, a proteolytic fragment of brain angiogenesis inhibitor 1, is an antiangiogenic and antitumorigenic factor. *Oncogene*. 2005; 24(22):3632–42. Epub 2005/03/23. 10.1038/sj.onc.1208317 [PubMed: 15782143]
 20. Hasegawa K, Nakamura T, Harvey M, Ikeda Y, Oberg A, Figini M, et al. The use of a tropism-modified measles virus in folate receptor-targeted virotherapy of ovarian cancer. *Clinical cancer research: an official journal of the American Association for Cancer Research*. 2006; 12(20 Pt 1):6170–8. Epub 2006/10/26. CCR-06-0992. 10.1158/1078-0432 [PubMed: 17062694]
 21. Geraghty RJ, Krummenacher C, Cohen GH, Eisenberg RJ, Spear PG. Entry of alpha herpesviruses mediated by poliovirus receptor-related protein 1 and poliovirus receptor. *Science*. 1998; 280(5369):1618–20. [PubMed: 9616127]
 22. Warner MS, Geraghty RJ, Martinez WM, Montgomery RI, Whitbeck JC, Xu R, et al. A cell surface protein with herpesvirus entry activity (HveB) confers susceptibility to infection by mutants of herpes simplex virus type 1, herpes simplex virus type 2, and pseudorabies virus. *Virology*. 1998; 246(1):179–89. 10.1006/viro.1998.9218 [PubMed: 9657005]
 23. Uchida H, Chan J, Goins WF, Grandi P, Kumagai I, Cohen JB, et al. A double mutation in glycoprotein gB compensates for ineffective gD-dependent initiation of herpes simplex virus type

- 1 infection. *Journal of virology*. 2010; 84(23):12200–9.10.1128/JVI.01633-10 [PubMed: 20861246]
24. Terada K, Wakimoto H, Tyminski E, Chiocca EA, Saeki Y. Development of a rapid method to generate multiple oncolytic HSV vectors and their in vivo evaluation using syngeneic mouse tumor models. *Gene therapy*. 2006; 13(8):705–14.10.1038/sj.gt.3302717 [PubMed: 16421599]
 25. Aghi M, Rabkin S, Martuza RL. Effect of chemotherapy-induced DNA repair on oncolytic herpes simplex viral replication. *Journal of the National Cancer Institute*. 2006; 98(1):38–50. Epub 2006/01/05. 10.1093/jnci/djj003 [PubMed: 16391370]
 26. Chou TC. Drug combination studies and their synergy quantification using the Chou-Talalay method. *Cancer research*. 2010; 70(2):440–6. Epub 2010/01/14. CAN-09-1947. 10.1158/0008-5472 [PubMed: 20068163]
 27. Chou TC. Preclinical versus clinical drug combination studies. *Leukemia & lymphoma*. 2008; 49(11):2059–80. Epub 2008/11/21. 10.1080/10428190802353591 [PubMed: 19021049]
 28. Chou TC. Theoretical basis, experimental design, and computerized simulation of synergism and antagonism in drug combination studies. *Pharmacological reviews*. 2006; 58(3):621–81.10.1124/pr.58.3.10 [PubMed: 16968952]
 29. Kaur B, Brat DJ, Calkins CC, Van Meir EG. Brain angiogenesis inhibitor 1 is differentially expressed in normal brain and glioblastoma independently of p53 expression. *The American journal of pathology*. 2003; 162(1):19–27. Epub 2003/01/01. 10.1016/S0002-9440(10)63794-7 [PubMed: 12507886]
 30. RLOD, McCormick A, Mukhopadhyay A, Woodhouse LC, Moat M, Grundy A, et al. The use of ovarian cancer cells from patients undergoing surgery to generate primary cultures capable of undergoing functional analysis. *PLoS one*. 2014; 9(6):e90604.10.1371/journal.pone.0090604 [PubMed: 24603616]
 31. Viale G, Gambacorta M, Dell'Orto P, Coggi G. Coexpression of cytokeratins and vimentin in common epithelial tumours of the ovary: an immunocytochemical study of eighty-three cases. *Virchows Archiv A, Pathological anatomy and histopathology*. 1988; 413(2):91–101.
 32. Geisinger KR, Dabbs DJ, Marshall RB. Malignant mixed mullerian tumors. An ultrastructural and immunohistochemical analysis with histogenetic considerations. *Cancer*. 1987; 59(10):1781–90. [PubMed: 2435401]
 33. Craveiro V, Yang-Hartwich Y, Holmberg JC, Sumi NJ, Pizzonia J, Griffin B, et al. Phenotypic modifications in ovarian cancer stem cells following Paclitaxel treatment. *Cancer medicine*. 2013; 2(6):751–62.10.1002/cam4.115 [PubMed: 24403249]
 34. Shepherd TG, Theriault BL, Campbell EJ, Nachtigal MW. Primary culture of ovarian surface epithelial cells and ascites-derived ovarian cancer cells from patients. *Nature protocols*. 2006; 1(6):2643–9.10.1038/nprot.2006.328
 35. Theriault BL, Portelance L, Mes-Masson AM, Nachtigal MW. Establishment of primary cultures from ovarian tumor tissue and ascites fluid. *Methods Mol Biol*. 2013; 1049:323–36. Epub 2013/08/06. 10.1007/978-1-62703-547-7_24 [PubMed: 23913227]
 36. Saeki Y, Fraefel C, Ichikawa T, Breakefield XO, Chiocca EA. Improved helper virus-free packaging system for HSV amplicon vectors using an ICP27-deleted, oversized HSV-1 DNA in a bacterial artificial chromosome. *Molecular therapy: the journal of the American Society of Gene Therapy*. 2001; 3(4):591–601.10.1006/mthe.2001.0294 [PubMed: 11319922]
 37. Domcke S, Sinha R, Levine DA, Sander C, Schultz N. Evaluating cell lines as tumour models by comparison of genomic profiles. *Nature communications*. 2013; 4:2126.10.1038/ncomms3126
 38. Dunfield LD, Shepherd TG, Nachtigal MW. Primary culture and mRNA analysis of human ovarian cells. *Biological procedures online*. 2002; 4:55–61.10.1251/bpo34 [PubMed: 12734568]
 39. Cheema TA, Kanai R, Kim GW, Wakimoto H, Passer B, Rabkin SD, et al. Enhanced antitumor efficacy of low-dose Etoposide with oncolytic herpes simplex virus in human glioblastoma stem cell xenografts. *Clinical cancer research: an official journal of the American Association for Cancer Research*. 2011; 17(23):7383–93. Epub 2011/10/07. CCR-11-1762. 10.1158/1078-0432 [PubMed: 21976549]
 40. Kanai R, Wakimoto H, Martuza RL, Rabkin SD. A novel oncolytic herpes simplex virus that synergizes with phosphoinositide 3-kinase/Akt pathway inhibitors to target glioblastoma stem

- cells. *Clinical cancer research: an official journal of the American Association for Cancer Research*. 2011; 17(11):3686–96. Epub 2011/04/21. CCR-10-3142. 10.1158/1078-0432 [PubMed: 21505062]
41. Okemoto K, Kasai K, Wagner B, Haseley A, Meisen H, Bolyard C, et al. DNA demethylating agents synergize with oncolytic HSV1 against malignant gliomas. *Clinical cancer research: an official journal of the American Association for Cancer Research*. 2013; 19(21):5952–9. CCR-12-3588. 10.1158/1078-0432 [PubMed: 24056786]
 42. Benencia F, Courreges MC, Conejo-Garcia JR, Buckanovich RJ, Zhang L, Carroll RH, et al. Oncolytic HSV exerts direct antiangiogenic activity in ovarian carcinoma. *Human gene therapy*. 2005; 16(6):765–78. Epub 2005/06/18. 10.1089/hum.2005.16.765 [PubMed: 15960607]
 43. Nawa A, Nozawa N, Goshima F, Nagasaka T, Kikkawa F, Niwa Y, et al. Oncolytic viral therapy for human ovarian cancer using a novel replication-competent herpes simplex virus type I mutant in a mouse model. *Gynecologic oncology*. 2003; 91(1):81–8. Epub 2003/10/08. [PubMed: 14529666]
 44. Nakamori M, Fu X, Meng F, Jin A, Tao L, Bast RC Jr, et al. Effective therapy of metastatic ovarian cancer with an oncolytic herpes simplex virus incorporating two membrane fusion mechanisms. *Clinical cancer research: an official journal of the American Association for Cancer Research*. 2003; 9(7):2727–33. Epub 2003/07/12. [PubMed: 12855653]
 45. Pasieka TJ, Baas T, Carter VS, Proll SC, Katze MG, Leib DA. Functional genomic analysis of herpes simplex virus type 1 counteraction of the host innate response. *Journal of virology*. 2006; 80(15):7600–12. Epub 2006/07/15. 10.1128/JVI.00333-06 [PubMed: 16840339]
 46. Alexander DE, Ward SL, Mizushima N, Levine B, Leib DA. Analysis of the role of autophagy in replication of herpes simplex virus in cell culture. *Journal of virology*. 2007; 81(22):12128–34. 10.1128/JVI.01356-07 [PubMed: 17855338]
 47. Harland J, Dunn P, Cameron E, Conner J, Brown SM. The herpes simplex virus (HSV) protein ICP34.5 is a virion component that forms a DNA-binding complex with proliferating cell nuclear antigen and HSV replication proteins. *Journal of neurovirology*. 2003; 9(4):477–88. Epub 2003/08/09. 10.1080/13550280390218788 [PubMed: 12907392]
 48. Roizman B, Markovitz N. Herpes simplex virus virulence: the functions of the gamma (1)34.5 gene. *Journal of neurovirology*. 1997; 3 (Suppl 1):S1–2. Epub 1997/05/01. [PubMed: 9179780]
 49. Rampling R, Cruickshank G, Papanastassiou V, Nicoll J, Hadley D, Brennan D, et al. Toxicity evaluation of replication-competent herpes simplex virus (ICP 34.5 null mutant 1716) in patients with recurrent malignant glioma. *Gene therapy*. 2000; 7(10):859–66. Epub 2000/06/14. [PubMed: 10845724]
 50. Kanai R, Rabkin SD, Yip S, Sgubin D, Zaupa CM, Hirose Y, et al. Oncolytic virus-mediated manipulation of DNA damage responses: synergy with chemotherapy in killing glioblastoma stem cells. *Journal of the National Cancer Institute*. 2012; 104(1):42–55. Epub 2011/12/17. 10.1093/jnci/djr509 [PubMed: 22173583]
 51. Singh SK, Clarke ID, Hide T, Dirks PB. Cancer stem cells in nervous system tumors. *Oncogene*. 2004; 23(43):7267–73. Epub 2004/09/21. 10.1038/sj.onc.1207946 [PubMed: 15378086]
 52. Zhuang X, Zhang W, Chen Y, Han X, Li J, Zhang Y, et al. Doxorubicin-enriched, ALDH(br) mouse breast cancer stem cells are treatable to oncolytic herpes simplex virus type 1. *BMC cancer*. 2012; 12:549. 10.1186/1471-2407-12-549 [PubMed: 23176143]
 53. Matsuda Y, Kure S, Ishiwata T. Nestin and other putative cancer stem cell markers in pancreatic cancer. *Medical molecular morphology*. 2012; 45(2):59–65. Epub 2012/06/22. 10.1007/s00795-012-0571-x [PubMed: 22718289]
 54. Campbell N, Greenaway J, Henkin J, Petrik J. ABT-898 induces tumor regression and prolongs survival in a mouse model of epithelial ovarian cancer. *Molecular cancer therapeutics*. 2011; 10(10):1876–85. Epub 2011/08/17. MCT-11-0402. 10.1158/1535-7163 [PubMed: 21844212]
 55. Greenaway J, Henkin J, Lawler J, Moorehead R, Petrik J. ABT-510 induces tumor cell apoptosis and inhibits ovarian tumor growth in an orthotopic, syngeneic model of epithelial ovarian cancer. *Molecular cancer therapeutics*. 2009; 8(1):64–74. Epub 2009/01/14. MCT-08-0864. 10.1158/1535-7163 [PubMed: 19139114]

56. Baker LH, Rowinsky EK, Mendelson D, Humerickhouse RA, Knight RA, Qian J, et al. Randomized, phase II study of the thrombospondin-1-mimetic angiogenesis inhibitor ABT-510 in patients with advanced soft tissue sarcoma. *Journal of clinical oncology: official journal of the American Society of Clinical Oncology*. 2008; 26(34):5583–8.10.1200/JCO.2008.17.4706 [PubMed: 18981463]
57. Ebbinghaus S, Hussain M, Tannir N, Gordon M, Desai AA, Knight RA, et al. Phase 2 study of ABT-510 in patients with previously untreated advanced renal cell carcinoma. *Clinical cancer research: an official journal of the American Association for Cancer Research*. 2007; 13(22 Pt 1): 6689–95. CCR-07-1477. 10.1158/1078-0432 [PubMed: 18006769]
58. Adusumilli PS, Chan MK, Chun YS, Hezel M, Chou TC, Rusch VW, et al. Cisplatin-induced GADD34 upregulation potentiates oncolytic viral therapy in the treatment of malignant pleural mesothelioma. *Cancer biology & therapy*. 2006; 5(1):48–53. Epub 2005/11/19. [PubMed: 16294031]
59. Bennett JJ, Adusumilli P, Petrowsky H, Burt BM, Roberts G, Delman KA, et al. Up-regulation of GADD34 mediates the synergistic anticancer activity of mitomycin C and a gamma134.5 deleted oncolytic herpes virus (G207). *FASEB journal: official publication of the Federation of American Societies for Experimental Biology*. 2004; 18(9):1001–3. Epub 2004/04/03. 10.1096/fj.02-1080fje [PubMed: 15059970]
60. Mahller YY, Williams JP, Baird WH, Mitton B, Grossheim J, Saeki Y, et al. Neuroblastoma cell lines contain pluripotent tumor initiating cells that are susceptible to a targeted oncolytic virus. *PLoS one*. 2009; 4(1):e4235.10.1371/journal.pone.0004235 [PubMed: 19156211]
61. Toyoizumi T, Mick R, Abbas AE, Kang EH, Kaiser LR, Molnar-Kimber KL. Combined therapy with chemotherapeutic agents and herpes simplex virus type 1 ICP34.5 mutant (HSV-1716) in human non-small cell lung cancer. *Human gene therapy*. 1999; 10(18):3013–29.10.1089/10430349950016410 [PubMed: 10609661]

Translational Relevance

Ovarian cancer is the 5th most deadly cancer in women, and two-thirds of women present with disease that has already metastasized to abdominal organs. While many women show disease regression after standard therapy of carboplatin and/or paclitaxel, nearly 70% recur. Recurrent tumors are often resistant to first-line therapeutics which may be due to a reservoir of chemotherapy-resistant stem-like cells that survive therapy, and reinitiate aggressive tumor growth. Here we describe anti-tumor efficacy of oncolytic herpes simplex virus (oHSV) 34.5ENVE against nestin-positive ovarian cancer stem-like cells. Further, this study shows improved anti-tumor efficacy when 34.5ENVE is combined with doxorubicin both *in vitro* and *in vivo*. Doxorubicin-based therapies are frequently administered to patients with recurrent ovarian cancer, and this study underscores the significance of combining oHSV with doxorubicin for patients who have developed resistance to primary chemotherapy.

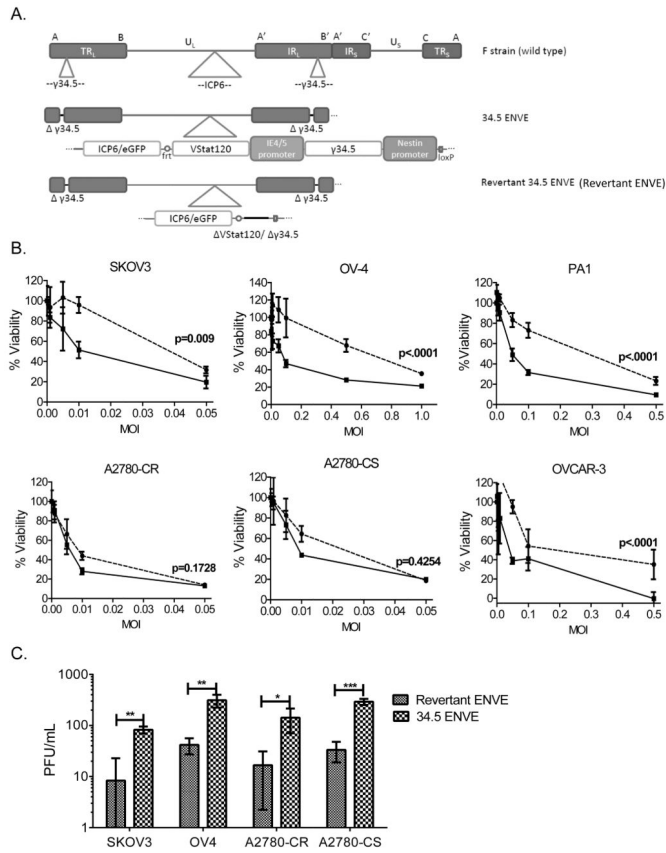


Figure 1. Efficacy of 34.5ENVE against OvCa cell lines *in vitro*. (A) Schematic of genetic alterations in the genomes of the oncolytic viruses used in the study, compared to wild type parental F strain HSV-1. TR, terminal repeats; IR, internal repeats; U, unique region; L, long; S, short; VStat120, Vasculostatin-120. (B) Cytotoxicity assay of panel of OvCa cell lines infected with 34.5ENVE (solid line, ■) or revertant ENVE (dotted line, ●) at increasing multiplicity of infection (MOI). Viability was assessed 3 days after treatment using MTT assay. Data shown are % viable cells relative to untreated control; error bars indicate standard deviation. Linear models were used to compare the means of two groups. P values shown represent the overall test result by linear models for the comparison between 34.5ENVE and revertant ENVE across all MOI levels. (C) Replication assay comparing 34.5ENVE and revertant ENVE in a panel of OvCa cell lines. Cells were infected at a low MOI, and cell lysates and media were harvested after 3 days. Viral titer was determined by standard plaque assay. Data shown are plaque-forming units (PFU)/mL; error bars indicate standard deviation (students t test; *, p<0.05; **, p<0.001; ***, p<0.0001.)

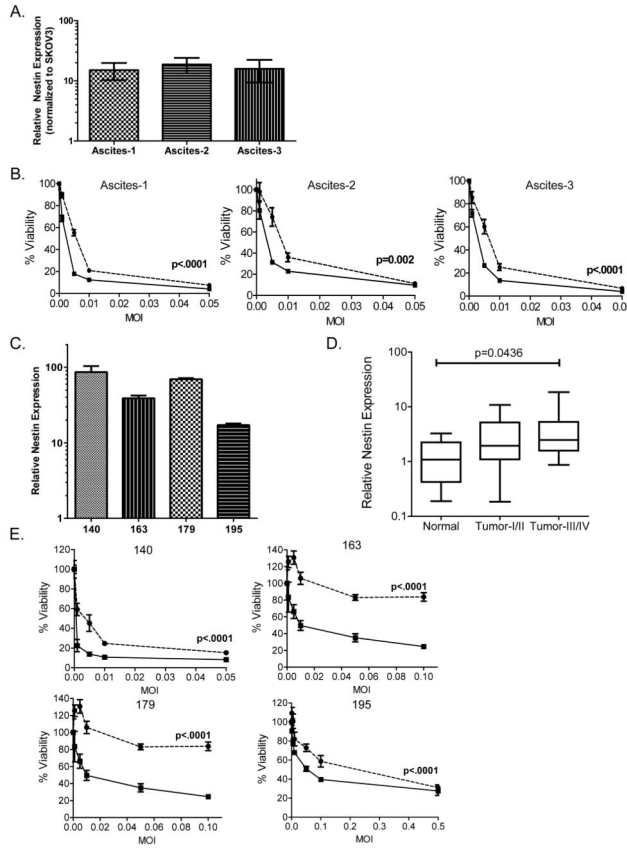
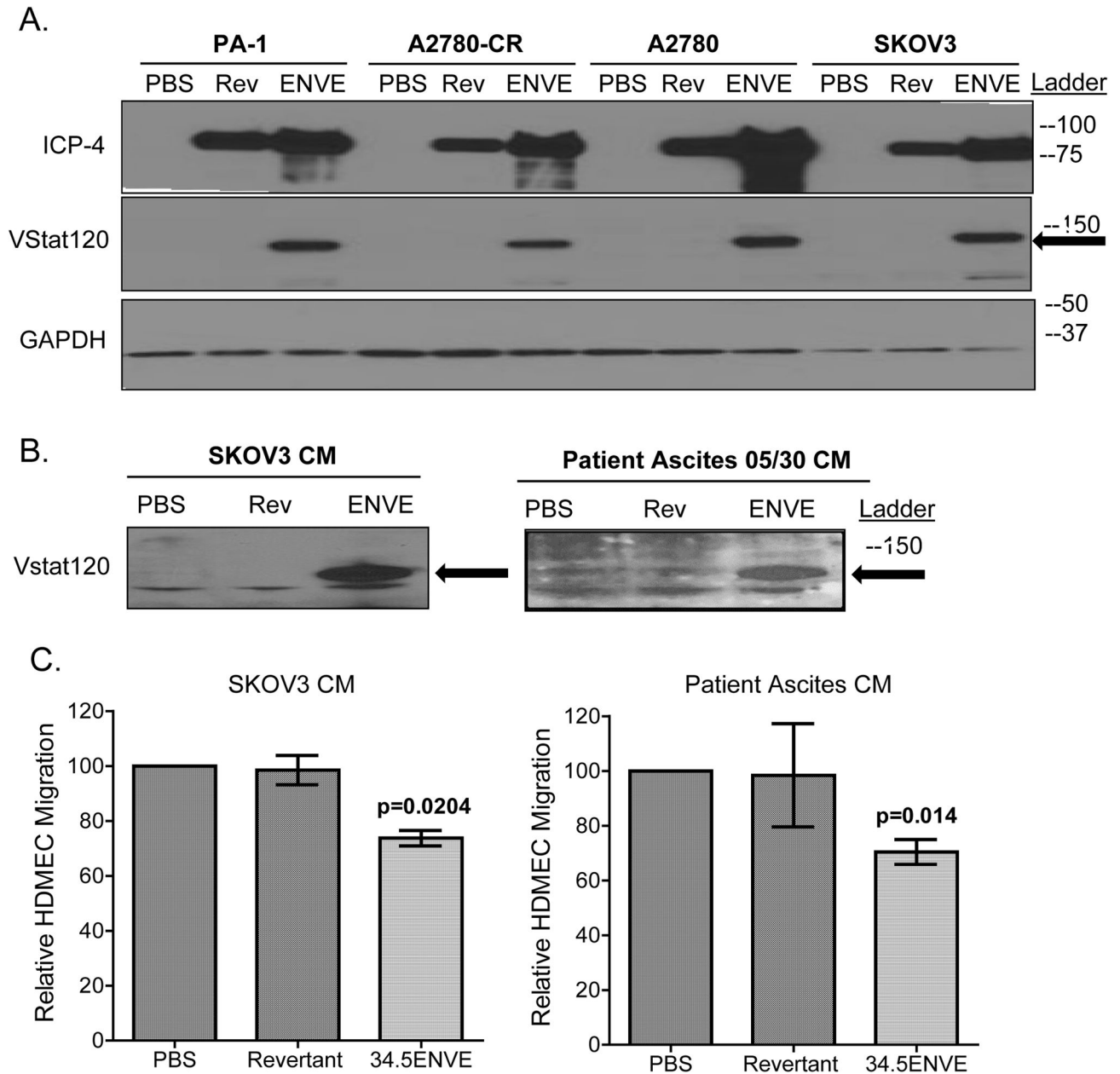


Figure 2. Increased sensitivity of nestin-positive experimental murine ascites- and patient ascites-derived tumor cells to oncolytic virus (OV) *ex vivo*. (A) Ascites-derived SKOV3 cells isolated from the experimental model of ovarian cancer have elevated nestin expression compared to SKOV3 cells grown *in vitro*. Data shown are nestin expression from three mouse isolates (ascites-1, ascites-2 and ascites-3) normalized to SKOV3 grown *in vitro*; error bars indicate standard deviation. (B) Murine ascites-derived SKOV3 tumor cells were tested for sensitivity to 34.5ENVE- (solid line, ■) and revertant ENVE-mediated (dotted line, ●) cytotoxicity. Cells were infected at increasing MOI, and viability was assessed 3 days after treatment using MTT assay. Data shown are % viable cells relative to untreated cells; error bars indicate standard deviation. Linear models were used to compare the means of two groups. P values shown represent the overall test result by linear models for the comparison between 34.5ENVE and revertant ENVE across all MOI levels.(C) Nestin expression is elevated in patient ascites-derived tumor cells. Data shown are nestin expression levels from four patient-derived ovarian cancer isolates (de-identified patient numbers 140, 163, 179, 195), normalized to normal ovarian tissue samples (from patients with endometriosis, carcinoma of the bladder, or leiomyoma of the myometrium; n=6); error bars indicate standard deviation. (D) Nestin expression increases as ovarian cancer tumor grade increases, as indicated in 48 human samples. Tissue Scan Disease Panel contained 48 samples from pathologist-verified ovarian cancer tissue cDNA including 6 normal, 14 Stage I, 5 Stage II, 22 Stage III and 1 Stage IV samples. Samples were tested for nestin expression,

and normalized to beta actin. Data shown is a box-and-whisker plot; ANOVA models were used to compare the mean of multiple groups (p value adjusted by Holm's procedure). (E) Patient ascites-derived ovarian cancer cells were tested for sensitivity to 34.5ENVE- (solid line, ■) and revertant ENVE-mediated (dotted line, ●) cytotoxicity. Cells were infected at increasing MOI, and viability was assessed 3 days after treatment using MTT assay. Data shown are % viable cells relative to untreated controls; error bars indicate standard deviation. Linear models were used to compare the means of two groups. P values shown represent the overall test result by linear models for the comparison between 34.5ENVE and revertant ENVE across all MOI levels.

**Figure 3.**

Vasculostatin-120 (Vstat120) is secreted by OvCa cells infected with 34.5ENVE, and conditioned media from 34.5ENVE-infected OvCa reduces endothelial cell migration *in vitro*. (A) Immunoblot of the indicated OvCa cell lysates harvested 24 hours after infection with 34.5ENVE (“ENVE;” at MOI=0.1), revertant ENVE (“Rev;” at MOI=0.1), or PBS. Blots were probed for expression of VStat120 (indicated with arrow), viral infected cell protein 4 (ICP4), and cellular GAPDH. Ladder indicates position. (B) Immunoblot of concentrated conditioned media from SKOV3. ip1 or patient ascites-derived tumor cells (number 140), harvested and concentrated 12 hours after infection with 34.5ENVE (“ENVE;” MOI= 2), revertant ENVE (“Rev;” MOI= 2), or PBS. Blot was probed for

Vstat120 (indicated with arrow). Ladder indicates position of molecular weight markers.(C) Migration of human dermal microvascular endothelial cells (HDMEC) treated with concentrated conditioned media (CM) collected from OvCa cells infected with 34.5ENVE, revertant ENVE or PBS for 12 hours. Media from infected SKOV3 or patient ascites-derived tumor cells (number 140) was collected and concentrated, and added to bottom chamber of a transwell assay; HDMEC were seeded on top of the membrane in the upper chamber. HDMEC migration was assessed by quantifying number of cells that had migrated through the membrane pores 12 hours after seeding. Data shown are mean number of cells migrated through membrane relative to control; error bars indicate standard deviation. ANOVA models used to compare the mean of multiple groups; p value adjusted by Holm's procedure.

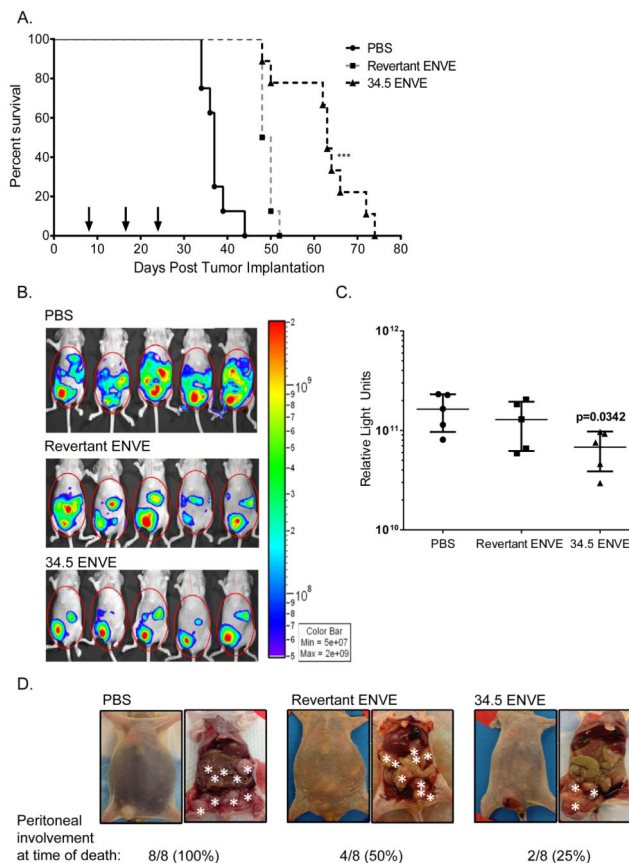


Figure 4.

Antitumor efficacy of 34.5ENVE against experimental model of disseminated peritoneal ovarian cancer. (A) OV therapy prolongs survival in experimental model of ovarian cancer. Mice were treated with 3 injections of 5×10^5 plaque-forming units (PFU) of virus (indicated by arrows) on days 8, 16 and 23 post tumor cell implantation. Data shown are Kaplan-Meier survival curves of the different treatment groups. Median survival of PBS-treated mice was 37 days, revertant ENVE was 49 days, and 34.5ENVE treatment extended survival to 63 days. Both OV therapies significantly prolonged survival, with an increased survival advantage in mice treated with 34.5ENVE compared to revertant ENVE. Survival curves compared among groups by Log rank test. ($p < 0.0001$). (B) OV therapy reduced tumor burden as indicated by bioluminescent signal. Bioluminescent imaging of representative mice show tumor burden in animals treated with PBS, revertant ENVE and 34.5ENVE twenty-eight days after tumor implantation. (C) Data shown are average relative quantification of luminescent output (relative light units in photons/second) twenty-eight days after tumor implantation; error bars indicate standard deviation. ANOVA models used to compare the mean of multiple groups; p value adjusted by Holm's procedure. (D) Necropsy images of representative mice from each treatment group. 34.5ENVE-treated animals displayed reduced disseminated peritoneal disease as indicated by reduced intraperitoneal tumor nodule seeding, and lack of ascites at time of death. Asterisks indicate subcutaneous tumor at site of injection and intraperitoneal tumors. Gross histology indicated that only two out of eight 34.5ENVE-treated mice had disseminated peritoneal disease at the

time of death. All eight PBS-treated mice, and four of eight revertant ENVE-treated mice displayed peritoneal seeding at time of death.

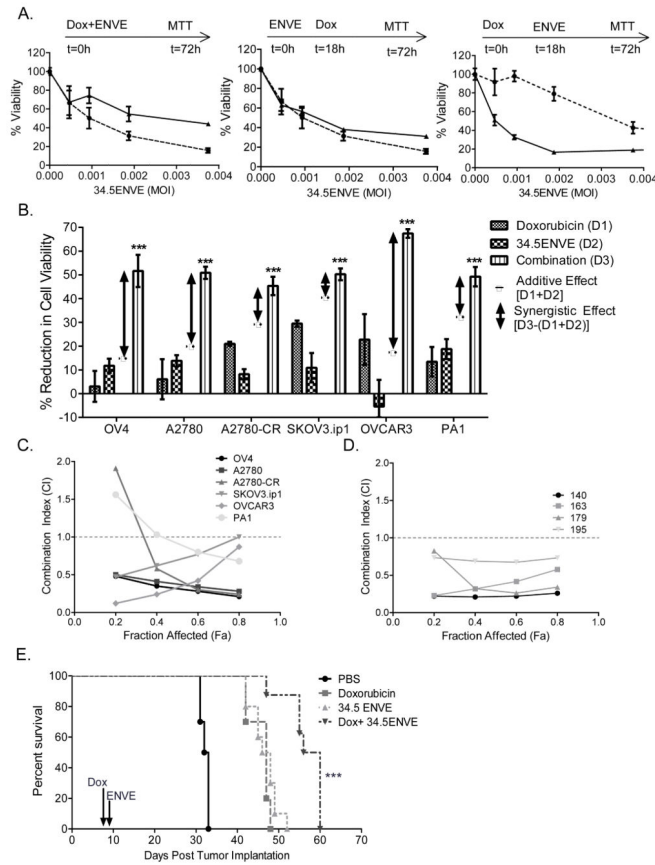


Figure 5. Synergistic killing of ovarian cancer cells treated with doxorubicin and 34.5ENVE *in vitro* and *in vivo*. (A) Doxorubicin treatment followed by 34.5ENVE is established as dosing regimen. Cytotoxicity assay of SKOV3-infected with 34.5ENVE alone (dotted line, ●) at increasing MOI, or in combination with doxorubicin (solid line, ▲) using different treatment schedules. Briefly, cells were treated with a fixed concentration of doxorubicin (100 nM) and with varying doses of 34.5ENVE administered 18 hours before doxorubicin, at the same time, or 18 hours after doxorubicin. MOI was calculated based on number of cells plated at t=0 hours. Viability was assessed 3 days after treatment using MTT assay. Data shown are % viable cells relative to untreated cells; error bars indicate standard deviation. Linear models were used to compare the means of two groups. $P < 0.001$; p values represents the overall test result by linear models for the comparison between 34.5ENVE and 34.5ENVE with doxorubicin across all MOI levels. (B) Combination therapy with doxorubicin and 34.5ENVE significantly increased cell death, as compared to either therapeutic alone. Briefly, the indicated cells were treated with sub-lethal doses of doxorubicin for 18 hours, followed by treatment with sub-lethal doses of 34.5ENVE. Cell viability was measured 3 days after treatment with 34.5ENVE via MTT. Data shown are % reduction in cell viability relative to untreated controls; error bars indicate standard deviation. Reduction in viability by either agent alone was quantified (called D1 for doxorubicin and D2 for 34.5ENVE). Reduction in viability by combination of doxorubicin and 34.5ENVE treatment was quantified (called D3). Additive effect was calculated as $[D1+D2]$; dashed line]. Synergistic

effect was calculated as $[D3-(D1+D2)]$; double-headed arrow]. In all 6 ovarian cancer cell lines, treatment of cells with both 34.5ENVE and doxorubicin resulted in more-than-additive cell killing. Two-way ANOVA models with the interaction term were used to evaluate the synergistic effect between two treatments (e.g. doxorubicin and 34.5ENVE; ***, $p<0.001$). Chou-Talalay combination interaction analysis of ovarian cancer cell lines (C) and primary patient ascites derived cells (D) treated with doxorubicin and 34.5ENVE. Briefly, the ED50 of doxorubicin and 34.5ENVE were each defined as the dosage yielding 50% cell viability at 72 hours following treatment. To evaluate if the combination resulted in synergistic cell killing, cells were treated with doxorubicin followed by drug wash out, and then infected with 34.5ENVE at serially diluted concentrations in a constant ratio. Cell viability was measured 72 hours after infection, and this data was used to establish a combination index (CI) using the CompuSyn program. Data shown in (C) and (D) are CI values at various fractions affected (Fa) for indicated cells. A $CI<1$ indicates synergistic interaction, whereas $CI>1$ is antagonistic and $CI=1$ is additive (dotted line). (E) Kaplan-Meier survival curve of doxorubicin, 34.5ENVE or combination treatment in the murine model of ovarian cancer. Mice bearing intraperitoneal SKOV3 cells were treated with one injection of doxorubicin ($10\mu\text{g}/\text{gram}$ body weight) eight days post tumor cell implantation, followed by treatment with a single injection of 34.5ENVE (5×10^5 PFU/mouse) one day later. Data shown are Kaplan-Meier survival curves of the different treatment groups. Median survival of PBS-treated mice was 32.5 days, doxorubicin-treated was 47 days, 34.5ENVE-treated was 47 days, and combination therapy of doxorubicin and 34.5ENVE extended median survival to 58 days (survival curves compared among groups by Log rank test; $p<0.001$).

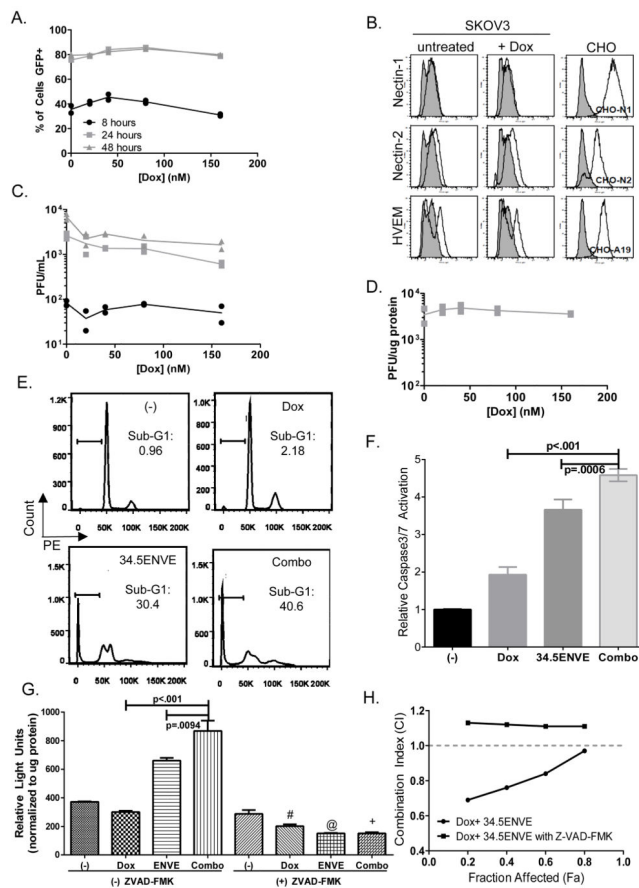


Figure 6.

Combination therapy with 34.5ENVE and doxorubicin increased apoptosis without altering virus replication in ovarian cancer cells. (A) Doxorubicin does not affect virus entry into cells as evaluated by measuring GFP-positive SKOV3 using flow cytometry. Cells were pretreated with doxorubicin for 18 hours, followed by wash out. Cells were then infected with 34.5ENVE at an MOI of 0.001 for 2 hours, followed by wash out of unbound virions. 8, 24 and 48 hours post-infection cells were harvested and fixed, and % GFP-positive infected cells was assessed by FACS. Data shown is % GFP-positive cells at each indicated time point from two replicates per treatment (black ●, 8 hours post-infection; light grey ■, 24 hours post-infection; dark grey ▲, 48 hours post-infection.) (B) Doxorubicin treatment does not alter HSV-1 receptor profile on SKOV3 cells. SKOV3 were harvested 18 hours after treatment with or without 40 nM doxorubicin, and HSV-1 receptor expression was evaluated using antibodies against nectin-1, nectin-2, herpes virus entry mediator (HVEM). Flow cytometry analysis indicated no change in expression of receptors in doxorubicin-treated sample as compared to untreated control. CHO cells expressing indicated HSV-1 receptors served as positive staining controls (CHO-N1, nectin-1; CHO-N2, nectin-2; CHO-A19, HVEM). (C) Virus replication assay indicates that doxorubicin does not increase viral replication. SKOV3 cells were treated with doxorubicin at indicated concentrations. Cells were then infected with 34.5ENVE at a low MOI=0.001 for two hours, followed by wash out of unbound virions. Cell lysate was harvested at indicated time points, and plaque-forming units (PFU) were quantified on Vero cells. Data shown is PFU per mL from each of

two replicates (black ●, 8 hours post-infection; light grey ■, 24 hours post-infection; dark grey ▲, 48 hours post-infection.) (D) Virus burst assay indicates that doxorubicin does not increase the number of viral particles produced in a single replication cycle. SKOV3 cells were treated with doxorubicin at indicated concentrations. Cells were then infected with 34.5ENVE at a high MOI=1 for two hours, followed by wash out of unbound virions. Cell lysate was harvested 24 hours after infection, and plaque-forming units (PFU) were quantified on Vero cells. Data shown is PFU per μg protein from two replicates. (E) Cell cycle analysis of cells treated with doxorubicin, 34.5ENVE or combination. Briefly, cells were treated with doxorubicin for 18 hours, followed by drug wash out. Cells were then infected with 34.5ENVE for 24 hours, and fixed via ethanol fixation, and stained with DNA dye PE to indicate DNA content. Sub-G1 fraction based on untreated G1 peak. Upper left panel, untreated, (“(-)”). Upper right panel, doxorubicin alone (“Dox,” 40 nM). Lower left panel, 34.5ENVE alone (“34.5ENVE,” MOI=0.02). Lower right panel, doxorubicin with 34.5ENVE (“Combo”). Data is representative flow cytometry image. (F) Caspase-3/7 activity is increased in SKOV3 treated with a combination of doxorubicin and 34.5ENVE, compared to single agent treatment. Briefly, SKOV3 were treated 160 nM doxorubicin for 18 hours followed by wash-out, followed by 34.5ENVE at an MOI of 0.04 for 24 hours. Caspase 3/7 activation is analyzed by luciferase activity (relative light units, RLU). Data shown are mean RLU per μg protein from cells treated with doxorubicin, 34.5ENVE or combination (ANOVA models used to compare the mean of multiple groups; p value adjusted by Holm’s procedure). (G) Treatment with pan-caspase inhibitor ZVAD-FMK blocks caspase 3/7 activation in SKOV3 cells treated with doxorubicin and 34.5ENVE. Cells treated with doxorubicin with or without virus were analyzed for caspase-3/7 activity in the presence or absence of ZVAD-FMK. The data shown are mean RLU per μg protein (ANOVA models used to compare the mean of multiple groups; p value adjusted by Holm’s procedure; “#,” $p < 0.001$ between dox without ZVAD-FMK and dox +ZVAD-FMK; “@,” $p < 0.0001$ between 34.5ENVE without ZVAD-FMK and 34.5ENVE +ZVAD-FMK; “+,” $p < 0.0001$ between combination without ZVAD-FMK and combination +ZVAD-FMK.) (H) Chou-Talalay analysis of interaction between doxorubicin and 34.5ENVE in SKOV3 in the presence or absence of caspase inhibitor ZVAD-FMK. Data shown are CI values at various fractions affected for indicated treatments. A $CI < 1$ indicates synergistic interaction, whereas $CI > 1$ is antagonistic and $CI = 1$ is additive.